The Egyptian Journal of Remote Sensing and Space Sciences xxx (2016) xxx–xxx

HOSTED BY

Contents lists available at ScienceDirect

The Egyptian Journal of Remote Sensing and Space Sciences

journal homepage: www.sciencedirect.com

Landform classification using a sub-pixel spatial attraction model to increase spatial resolution of digital elevation model (DEM)

Marzieh Mokarrama [a,*], Majid Hojati [b]

[a] Department of Range and Watershed, Agriculture College and Natural Resources of Darab, Shiraz University, Iran
[b] Department of Remote Sensing and GIS, Tehran University, Iran

ARTICLE INFO

Article history:
Received 24 July 2016
Revised 19 November 2016
Accepted 20 November 2016
Available online xxxx

Keywords:
Landform
TPI
DEM
Sub-pixel
Spatial resolution

ABSTRACT

The purpose of the present study is preparing a landform classification by using digital elevation model (DEM) which has a high spatial resolution. To reach the mentioned aim, a sub-pixel spatial attraction model was used as a novel method for preparing DEM with a high spatial resolution in the north of Darab, Fars province, Iran. The sub-pixel attraction models convert the pixel into sub-pixels based on the neighboring pixels fraction values, which can only be attracted by a central pixel. Based on this approach, a mere maximum of eight neighboring pixels can be selected for calculating of the attraction value. In the mentioned model, other pixels are supposed to be far from the central pixel to receive any attraction. In the present study by using a sub-pixel attraction model, the spatial resolution of a DEM was increased. The design of the algorithm is accomplished by using a DEM with a spatial resolution of 30 m (the Advanced Space borne Thermal Emission and Reflection Radiometer; (ASTER)) and a 90 m (the Shuttle Radar Topography Mission; (SRTM)). In the attraction model, scale factors of (S = 2, S = 3, and S = 4) with two neighboring methods of touching (T = 1) and quadrant (T = 2) are applied to the DEMs by using MATLAB software. The algorithm is evaluated by taking the best advantages of 487 sample points, which are measured by surveyors. The spatial attraction model with scale factor of (S = 2) gives better results compared to those scale factors which are greater than 2. Besides, the touching neighborhood method is turned to be more accurate than the quadrant method. In fact, dividing each pixel into more than two sub-pixels decreases the accuracy of the resulted DEM. On the other hand, in these cases DEM, is itself in charge of increasing the value of root-mean-square error (RMSE) and shows that attraction models could not be used for S which is greater than 2. Thus considering results, the proposed model is highly capable of increasing the spatial resolution of DEM (the new DEM with high spatial resolution). In the next step, in order to prepare the geomorphology map using topographic position index (TPI), the DEM with scale factor of (S = 2) was used, touching neighborhood serves as input. The landform classes were extracted by using TPI with the new DEM; consequently, the attraction model extraction showed details of landforms that make them more separable than the landform map prepared by utilizing the 90 m spatial resolution DEM. Moreover, the results showed that the landform of the 90 m spatial resolution DEM (S = 2, T = 2) and ASTER DEM 30 m were similar to each other, these results indicate a high accuracy of the proposed attraction model.

1. Introduction

The topographic maps, aerial stereo-photos, satellite imagery and digital elevation models (DEMs) were used as inputs for landform classification in the geomorphology science. In some recent researchers Concerning the landform classification, DEMs have been used in the following researches: (Atkinson, 2005; Burrough et al., 2000; MacMillan et al., 2000; Migoń et al., 2013; Mokarram and Danish, 2015; Mokarram et al., 2015; Saadat et al., 2008; Schmidt and Hewitt, 2004; Verhagen and Drâguţ, 2012) .

There are different methods for extracting landforms including the classification of terrain parameters (Dikau, 1989; Dikau et al., 1995), filter techniques (Sulebak et al., 1997), cluster analysis (Dikau, 1989; Dikau et al., 1995; Etzelmüller, 2000) multivariate

Peer review under responsibility of National Authority for Remote Sensing and Space Sciences.

* Corresponding author.
E-mail addresses: m.mokarram@shirazu.ac.ir (M. Mokarrama), majid.hojati@ut.ac.ir (M. Hojati).

http://dx.doi.org/10.1016/j.ejrs.2016.11.005
1110-9823/

statistics (Adediran et al., 2004); mathematical morphology (Guru and Dinesh, 2004) and multi-scale analysis of the digital elevation models (Mokarram et al., 2015). In gemorphologic researches, DEMs play a great role as the geographic information data base used for extracting basic components and terrain parameters.

One of the important properties of DEM is the spatial resolution which represents the accuracy of DEM (Takagi, 1998). Visually, the spatial resolution can change features derived from DEMs and thus can influence on models associated with them (Gallant and Hutchinson, 1997; Haile and Rientjes, 2005; Omer et al., 2003). There are many studies that uses DEMs with different resolutions (Hutchinson and Dowling, 1991; Jenson, 1991; Wolock and McCabe, 2000). Noticeably, there are some methods for increasing the spatial resolution of DEM. For example, an integration of the 2-D hydraulic model and the high-resolution LiDAR-derived DEM has been used for floodplain flow modeling (Shen et al., 2015). One model of increasing the spatial resolution is the attraction model that is based on the sub-pixel.

The sub-pixel algorithm divides a pixel into sub-pixels by considering the spatial dependence (Atkinson, 1997). This model treats a pixel as a combination of surrounding pixels which are affecting a central one based on their distance. The first linear optimization technique for sub-pixel mapping algorithm was introduced by (Verhoeye, 2002) and was inspired by Atkinson (1997).

The attraction model algorithm spatially depends on the neighborhoods of the central pixel which is attracted by surrounding sub-pixels. Another possibility is the hypothesis of sub-pixel interaction as introduced by Koen Mertens (2003) and Atkinson (2005). In order to reach at a pixel state with the maximum number of sub-pixels with identical neighboring classes, there are several methods such as the genetic algorithms and pixel swapping in which the initial pixel fraction values are considered as a constraint (Atkinson, 2005; Koen Mertens, 2003).

The present paper focuses on the landform classification by using the attraction model analysis of DEMs. In order to classify landforms, it is important to determine DEM with high resolution as the input data. The size and the space of landforms show clustering around the spatial resolution characteristic (Evans, 2012). The attraction model has always been used to increase the spatial resolution of satellite images (Atkinson, 1997; S et al., 2008; Verhoeye, 2002; Xu et al., 2013); however, There is not any study about this model which was performed regarding DEMs. In this study, authors applied a selected sub-pixel method to increase the spatial resolution and the accuracy of DEMs served as an input for landform classification in the areas of north of Darab, Fars province, Iran. The landform classification is performed by using a topographic position index (TPI). The generated landform maps via the attraction model DEM and the primary DEM (Shuttle Radar Topography Mission (SRTM)) were compared as well. Generally, the present used methodology is summarized as followings:

1. At first, the attraction model is run on SRTM DEM with spatial resolution of 90 m.
2. Then in the attraction model, the quadrant, touching methods and scale factors of 2, 3 and 4 are tested for each neighboring method.
3. After that, an RMSE index is calculated for each output of the attraction model and consequently the DEM with the lowest RMSE is selected.
4. Finally, the TPI model is applied to the original SRTM DEM. Besides, the extracted DEM from the attraction model is compared to the obtained result.

The Fig. 1 shows the general steps which has down in this study.

2. Material and methods

2.1. SRTM and ASTER GDEM

The joint Japanese–US Advanced Spaceborne Thermal Emission and Reflection Radiometer (ASTER) Global Digital Elevation Model (GDEM) version 2 was released in October 2011. Version 2 was released 3 years after version 1 by the Ministry of Economy, Trade and Industry (METI) of Japan cooperating with the United States National Aeronautics and Space Administration (NASA) (Rexer and Hirt, 2014). ASTER GDEM is the most complete mapping of the earth ever made, covering 99% of its surface. The elevation difference between SRTM and ASTER products was evaluated by using the root mean square error (RMSE) which was found to be less than 50 m (Nikolakopoulos, 2006).

Shuttle Radar Topography Mission (SRTM) is an international mission which is aimed to produce digital elevation models. SRTM consisted of a specially modified radar system that flew on board the Space Shuttle Endeavour during the 11-day STS-99 mission in February 2000. In order to get the acquire topographic data, the SRTM payload was outfitted with two radar antennae. The raw data are restricted for the government use. For the rest of the world, only three arcsecond (90 m) data are available (Nikolakopoulos, 2006).

However, some reviewers have commented that the true resolution is considerably lower than that and it is not as good as the SRTM data (Rexer and Hirt, 2014):

- ASTER GDEM data were downloaded from (http://gdem.ersdac.jspacesystems.or.jp) for free. Authors of the present study call it as a DEM 30 m.
- SRTM DEM data were downloaded from (http://srtm.usgs.gov) for free. Authors name it a DEM 90 m.
- Ground station points gathered from surveys were done by National Cartographic Center of Iran (NCC).

Preprocessing of DEMs were achieved by using ARCMAP version 10.3. An attraction model was achieved by using Matlab version 2013 R2.

2.2. Attraction sub-pixel model

A sub-pixel mapping was first introduced by Atkinson (1997). This method is used to extract a spatial distribution of various classes in a mixed pixel (Xu et al., 2014). The sub pixel method keeps a spatial dependence into account among sub-pixels in a pixel surrounded by other pixels (Atkinson, 1997). Attraction models are vastly used in geo-statistic studies (Mertens, 2008). These models can divide each mixed pixel into a set of sub pixel fractions and can locate different classes in a pixel.

In the present study two quadrant and touching neighboring methods are used. In the quadrant neighborhood, a neighbor pixel is the only pixel in the same quadrant whereas in the touching neighborhood, a neighbor pixel is defined as a pixel which physically touches a sub pixel. A sample of two neighborhood methods with different scale factors are shown in Fig. 2 (Mertens and Chawla, 2014) in which all the pixels which attract a sub-pixel are explained with the same color as the sub-pixel.

In attraction models, a scale factor (S) shows the number of sub-pixels in each central pixel. In the present paper, two neighborhood methods with S = 2, 3, 4 are examined.

It must be noticed that both neighboring methods are the same when S = 2. The aforementioned neighborhoods (Fig. 2) can now be formulated as (1)–(3) (Mertens and Chawla, 2014):

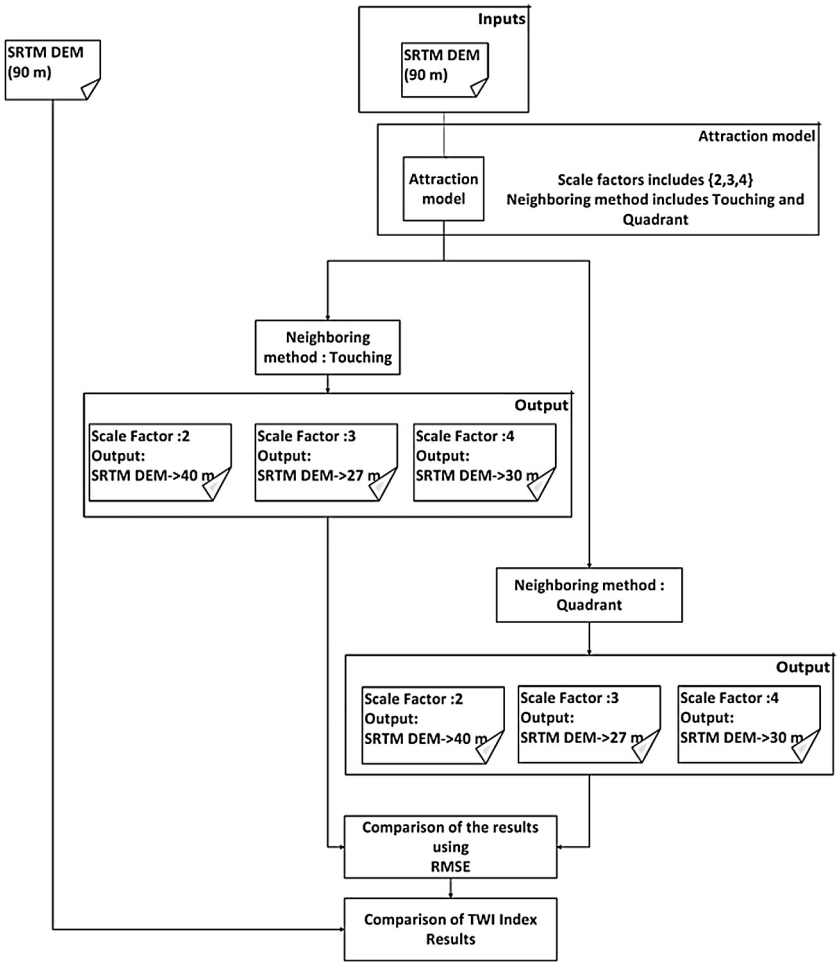

Fig. 1. flowchart for the methodology used in the study area to landform classification.

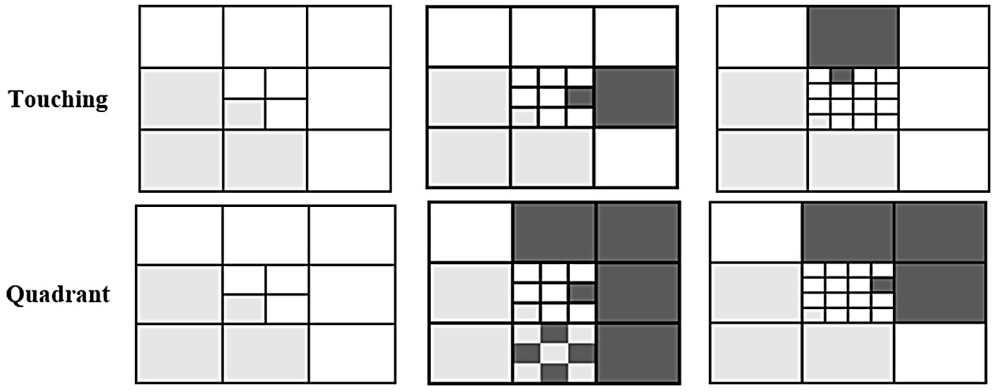

Fig. 2. Graphic of sub-pixel attraction model for different neighborhoods and scale factors adapted from Mertens and Chawla (2014).

N Touching neighborhood:

$$N_1[p_{a,b}] = \left\{ P_{i,j} | d(p_{a,b}, P_{i,j}) \leqslant \frac{S+1}{\sqrt{2}} \right\} \quad (1)$$

N Quadrant neighborhoods:

$$N_1[p_{a,b}] = \left\{ P_{i,j} | d(p_{a,b}, P_{i,j}) \leqslant \frac{2S+1}{\sqrt{2}} \right\} \quad (2)$$

With the distance defined as:

$$(p_{a,b}, P_{i,j}) = \sqrt{[a+0.5-S(i+0.5)]^2 + [b+0.5-S(j+0.5)]^2} \quad (3)$$

where Pi,j is a pixel which falls in the neighborhood of a specific sub pixel, pa,b. S can be the scale factor. I and j are the locations of each pixel in a 3 * 3 windows, and a and b are known as relative locations of each sub pixel in the central pixel. To define the coordinate systems more clearly, it is necessary to mention that distance (d) is calculated based on the Eqlidian distance.

Each neighboring method gives a different set of pixels which falls into a neighboring area of a specific sub pixel inside the central pixel. In the next step after choosing each pixel set for each sub-pixel, the attraction value for each pixel is calculated as Eq. (4).

$$p_{a;b}(c) = Avg\left\{\frac{P_{i;j}(c)}{d(p_{a;b} \cdot P_{i;j})} \mid P_{i;j} \in N_t[p_{a;b}]\right\} \quad (4)$$

where $P_{a;b(c)}$ is the attraction value for sub-pixel $p_{a;b,}$ class c. $P_{i;j(c)}$ is a fraction value for pixel $P_{i;j,}$class c. S is the scale factor, N_t[pa;b] is a neighborhood of type t of sub-pixel $p_{a;b}$, d($p_{a;b}$; Pi;j) is the distance from sub-pixel pa;b to pixel Pi;j in N_t[pa;b] neighborhood that can divide each fraction value of each class of N into its distance (d). In this study, a fraction value is assumed as a DN value of DEM raster or the elevation value.

After performing this stage, raw attraction values can be computed. These values can then be used to attach each sub-pixel proper class: Noticeably, classes with highest attractions are attached first.

The above algorithm is used to run the attraction model on a 3 * 3-pixel window in the MATLAB software with scale factors of 2, 3 and 4; besides, the neighborhood methods of 1 = touching, 2 = quadrant have been selected as well.

The sub-pixel mapping uses land cover classes around a pixel and estimates the values in each pixel. Here, authors used the attraction model algorithm, which is designed based on attraction values which are calculated concerning the distance and the classes' values to increase the spatial resolution of DEM. In this work, it is assumed that each elevation value in each window is a separate class. On the other hand, in each 3 * 3 window, each pixel is considered as a separate class and it is calculated, as well. An example of calculation for a sub-pixel is shown in the following tables (Fig. 3).

(a)

Pixel Value 1950	Pixel Value 1950	
Pixel Value 1700		

(b)

Disatance: 1.06066	Disatance 0.790569	
Disatance: 0.790569		

(c)

Attraction: 2152.527	Attraction 2152.527	
Attraction: 2150.349		

Fig. 3. An example of the attraction value calculation for a sub-pixel. (a) Represents pixel values in a touching or quadrant neighborhood, (b) shows the calculated distance between a sub-pixel and each pixel, and (c) is an attraction value of each surrounding pixel. The pixel value for a higher attraction value is the value of a sub-pixel.

2.3. Accuracy assessment

The accuracy is measured by comparing the output of the sub-pixel mapping with the ground station points which are gathered manually. The root mean square error (RMSE) is calculated for the artificial images. To Calculate RMSE, approximately 487 sample points from ground surveys are used in the study area applied in Eq. (5).

$$RMSE = \sqrt{\left(\frac{1}{N}\right)\sum_{i=1}^{N}\{z(X_i) - \hat{Z}(X_i)\}^2} \quad (5)$$

where $\hat{Z}(X_i)$ is the predicted value, z(xi) is considered the observed (known) value (the sample point from the ground surveys) and N indicates the number of values in the dataset (Johnston et al., 2001).

2.4. Topographic position index (TPI) for landform classification

For landform classification, the topographic position index (TPI) was used. TPI measures the height of each cell in a DEM to reach at the mean height of a determined neighborhood around that cell.

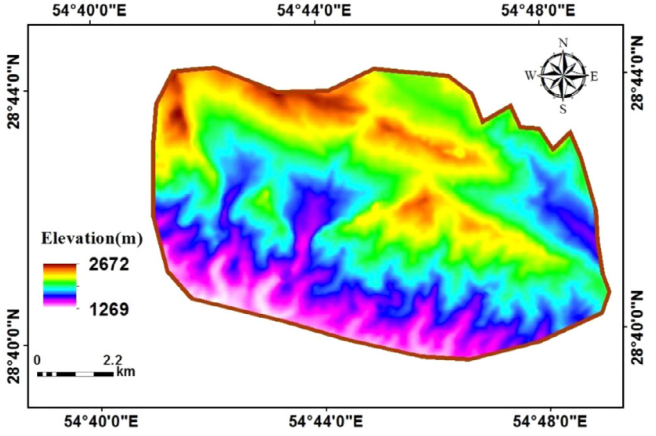

Fig. 4. Location of the study area (digital elevation model (DEM) with spatial resolution of 90 m).Source: http://earthexplorer.usgs.go.

Table 1
Variety of Landform classification based on TPI values. Source: Takagi (1998).

Number	Landform classes	Description	
		Small scales	Large scales
1	Canyons, deeply incised streams	Small Neighborhood: $T_o \leqslant -1$	Large Neighborhood: $T_o \leqslant -1$
2	Mid slope drainages, shallow valleys	Small Neighborhood: $T_o \leqslant -1$	Large Neighborhood: $-1 < T_o < 1$
3	Upland drainages, headwaters	Small Neighborhood: $T_o \leqslant -1$	Large Neighborhood: $T_o \geqslant 1$
4	U-shaped valleys	Small Neighborhood: $-1 < T_o < 1$	Large Neighborhood: $T_o \leqslant -1$
5	Plains small	Neighborhood: $-1 < T_o < 1$, Slope $\leqslant 5°$	Large Neighborhood: $-1 < T_o < 1$
6	Open slopes	Small Neighborhood: $-1 < T_o < 1$, Slope $> 5°$	Large Neighborhood: $-1 < T_o < 1$
7	Upper slopes, mesas	Small Neighborhood: $-1 < T_o < 1$	Large Neighborhood: $T_o \geqslant 1$
8	Local ridges/hills in valleys	Small Neighborhood: $T_o \geqslant 1$	Large Neighborhood: $T_o \leqslant -1$
9	Midslope ridges, small hills in plains	Small Neighborhood: $T_o \geqslant 1$	Large Neighborhood: $-1 < T_o < 1$
10	Mountain tops, high ridges	Small Neighborhood: $T_o \geqslant 1$	Large Neighborhood: $T_o \geqslant 1$

Mean height is subtracted from the elevation value at the center (Eq. (6)) (Weiss, 2001):

$$TPI_i = T_0 - \sum_{n-1} T_n / n \quad (6)$$

where;

T_0 = height of the model point under evaluation

T_n = height of grid

n = the total number of all-around points using in the height.

TPI values at small and large scales create different landforms (Takagi, 1998) (Table 1).

3. Study area

The study area (Darab, Fars province, Iran) has an area of about 126.1 km^2 and is located between the longitudes 28° 39′ to 28° 44′ N and the latitudes 54° 40′ and 54° 49′ E. Fig. 4 shows a Shuttle Radar Topography Mission (SRTM) DEM data of the study area. The altitude of the study area ranges from the lowest of 1159 m to the highest of 3006 m. The major crops at the study area are wheat, citrus, cotton, maize and palm. The average annual rainfall in the study area is 300 mm. The study area has warm days in summer with 38–46 °C and moderate winters with (15–25 °C) (Oryan et al., 1997; Rezaei and Shakoor, 2011).

4. Results and discussion

In order to investigate the spatial resolution enhancement of DEM 90 m, the attraction model was used. Results of the model for DEM 90 m are shown in Fig. 5. In order to find the best model for increasing the spatial resolution, three scales (2, 3, and 4) with two neighborhood methods of touching and quadrant were used. As it is shown in Fig. 5, with increasing the value of the scale factor, the sub-pixel increases; consequently, the information of sub-pixel increases more than the primary pixel and the elevation changes are well displayed. Surely with calculating RMSE, it is cleared that only scale factor 2 shows an increment in the accuracy and other scale factors do not show a trustworthy result. The reason justifies this is applying the elevation as the only input class in the attraction model. Therefore, it is concluded that any increase of the scale results in increasing in the spatial resolution. Furthermore, results show that the touching neighborhood (T1) revealed better results than the quadrant (T2) method, as the sum of the RMSE values for touching method was lower than that of the quadrant method. There is also a change in RMSE value of two DEMs such that for DEM 90 m it is around 0.32 m (6.06–6.39 = 0.32) which shows a slight improvement in the accuracy of DEMs with a better spatial resolution.

After producing output images for each neighborhood method, three scale factors of 2, 3 and 4 are obtained. Each image is

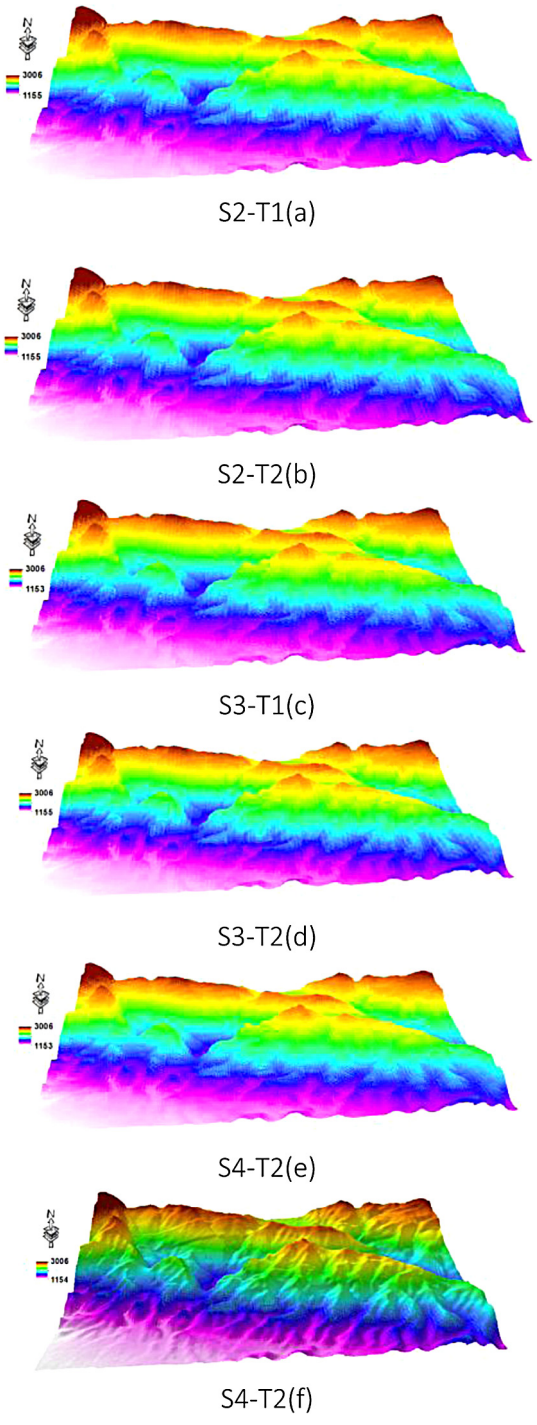

Fig. 5. DEMs generated using touching and Quadrant neighborhood with different scale factors. (a), (b) and (c) are the DEMs extracted from the quadrant neighboring method and scale factors of 2, 3 and 4 respectively; (d), (e) and (f) are extracted DEMs from the touching neighboring method and scale factors of 2, 3, and 4 respectively. As images show the maximum and minimum values are constant and only the number of pixels in each image is increased based on the scale factor.

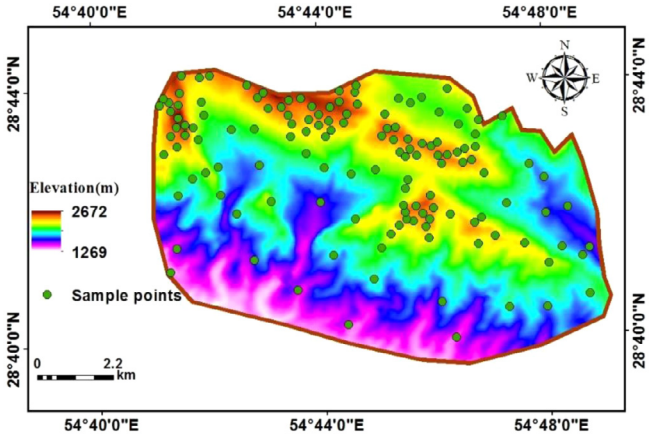

Fig. 6. The location of ground sample points by National Cartographic Center of Iran (NCC).

compared to the ground station points by using RMSE and accordingly results are compared. To make a quantitative evaluation of the generated DEMs with touching and Quadrant neighborhood methods, 487 points were selected from the ground station (Points are measured by National Cartographic Center of Iran (NCC)) (Fig. 6).

The Root Mean Square Errors (RMSE) of these points in each method of DEM 90 and DEM 30 m were calculated and presented in Table 2. In Fig. 6, the accuracy measures of two touching and quadrant neighborhood methods for different scale factors (2, 3, and 4) are shown as 3D of DEM 90 m. As depicted, the lowest RMSE value showed the best accuracy for increasing the spatial resolution.

Table 2
Output DEMs RMSE values (S = Scale factor, T1 = touching method, T2 = Quadrant method).

Output	RMSE
S = 2, T1	6.06
S = 3, T1	8.09
S = 4, T1	7.76
S = 2, T2	6.06
S = 3, T2	8.23
S = 4, T2	8.89

In fact with increasing the scale factor to the value of 2, the accuracy increases due to the decrease in the RMSE value; and when the value of scale factor increase to 3 and 4, the accuracy decreases; therefore, applying scale factors of 3 and 4 is not suitable.

In Fig. 7 the scatter plots of points which are extracted from attraction model and real elevation values which are extracted from land survey are shown. As results show the quadrant and touching methods have the same values when scale factor is equal to 2 and it also has the best estimation with lowest RMSE value.

The TPI and landform classification maps were generated by using the attraction model (S2, T2) and DEM 90 m which are shown in Fig. 6. There are differences between three methods of landform classification with different resolution. For the attraction model (Fig. 8), TPI is calculated between 141.84 to 190.8 for 5 * 5

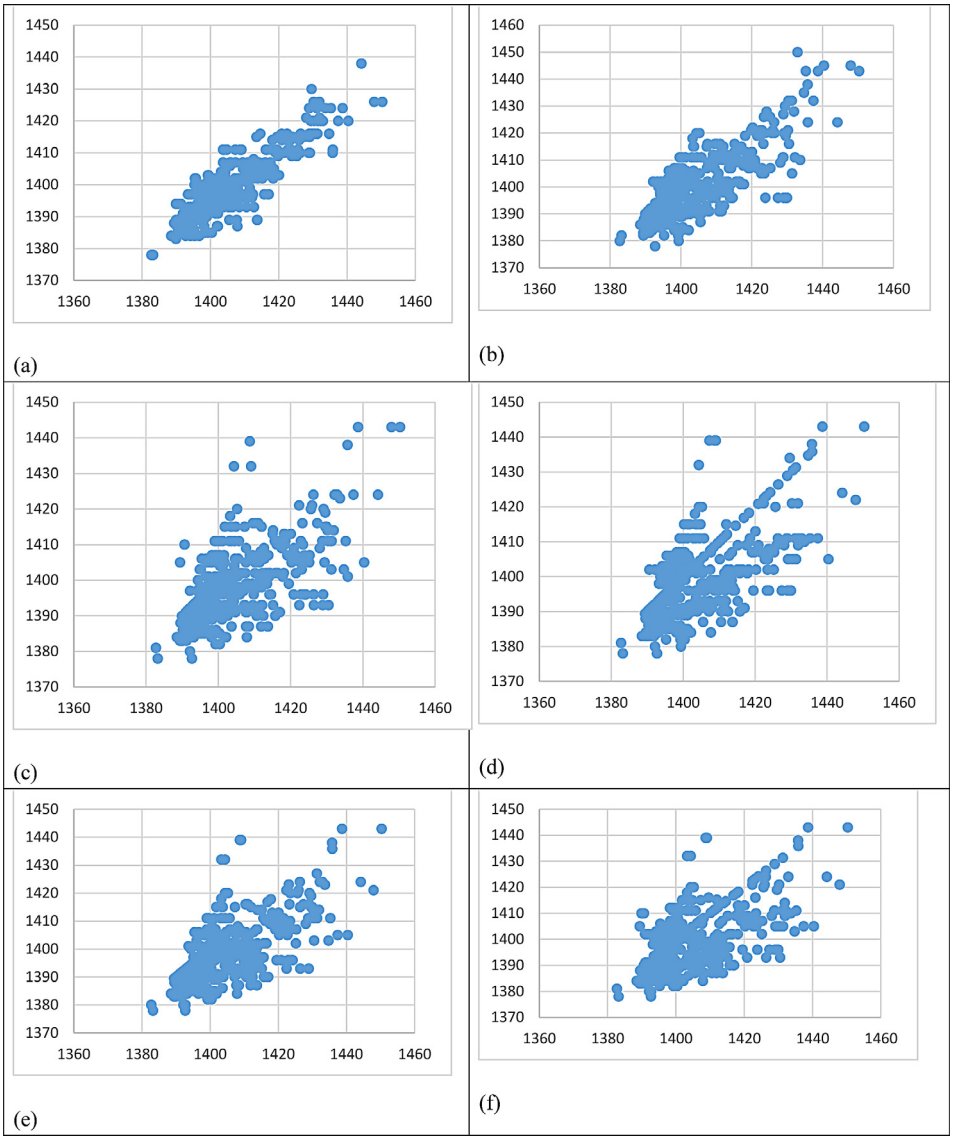

Fig. 7. Scatter plot of attraction model results and ground station data. (a) Dem 90 m data, (b) Scale factor 2 and touching and quadrant neighboring models, this two models have the same results when scale factor is equal to 2, (c) scale factor 3 and quadrant neighboring method, (d) scale factor 3 and touching neighboring method, (e) scale factor 4 and quadrant neighboring method, (f) scale factor 4 and touching neighboring method,

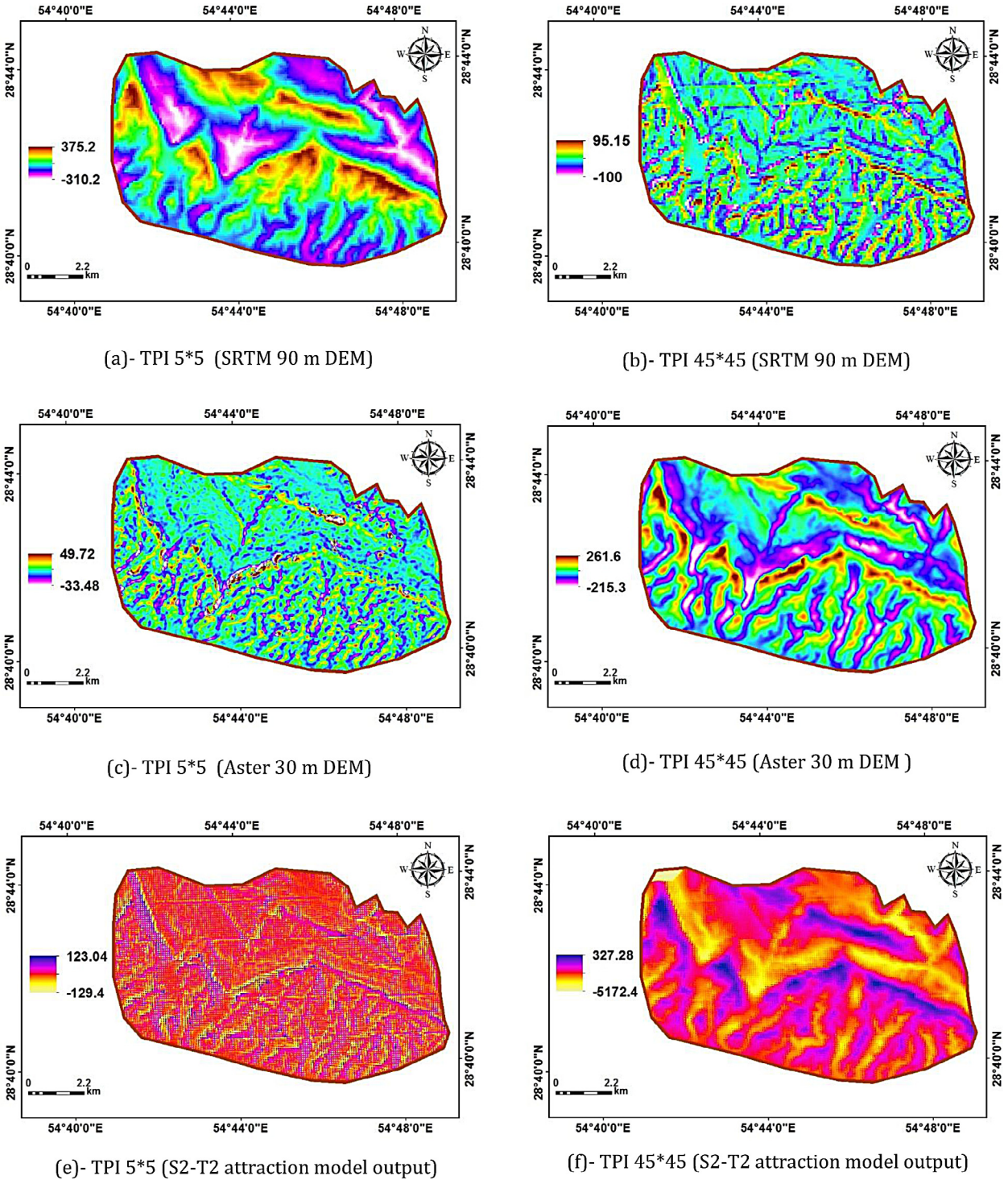

(a)- TPI 5*5 (SRTM 90 m DEM)

(b)- TPI 45*45 (SRTM 90 m DEM)

(c)- TPI 5*5 (Aster 30 m DEM)

(d)- TPI 45*45 (Aster 30 m DEM)

(e)- TPI 5*5 (S2-T2 attraction model output)

(f)- TPI 45*45 (S2-T2 attraction model output)

Fig. 8. TPI maps generated by using small and large neighborhoods which applied on the results of the attraction model, DEM 90 m of Shuttle Radar Topography Mission (SRTM). (a) And (b) show the results of TPI model which is applied on DEM 90 m with 5 * 5 windows size and 45 * 45 pixels windows size respectively; (c) And (d) are TPI results extracted from DEM 30 m and 5 * 5 windows size and 45 * 45 pixels windows size respectively; (e) and (f) are the results of TPI model which is applied on attraction models (T2-S2) result with 5 * 5 windows size and 45 * 45 pixels windows size respectively.

and −236.68 to 268.08 for 45 * 45 neighborhood, while the minimum TPI is between −107.33 to 95.15 and −310.25 to 437.86 for small and large neighborhoods of DEM 90 m, respectively. Finally in order to investigate the accuracy of the landform with the attraction model, DEM 30 m was used and compared to them. For DEM 30 m, TPI values are between −227.5 to 261.6 and −34.5 to 49.7 for large and small neighborhoods, respectively (Fig. 8).

The landform maps generated based on the TPI values of two DEMs are shown in Fig. 8. By comparing landforms extractions which are shown by using two methods (Fig. 8), it is observed that with increasing the spatial resolution, more details of the region are visible (Fig. 9).

Areas (%) of each class are shown in Fig. 10 and Table 3. In Fig. 10, results of TPI model on two SRTM DEM and attraction DEM are compared. At first, the area of each TPI model class for

Please cite this article in press as: Mokarrama, M., Hojati, M. Egypt. J. Remote Sensing Space Sci. (2016), http://dx.doi.org/10.1016/j.ejrs.2016.11.005

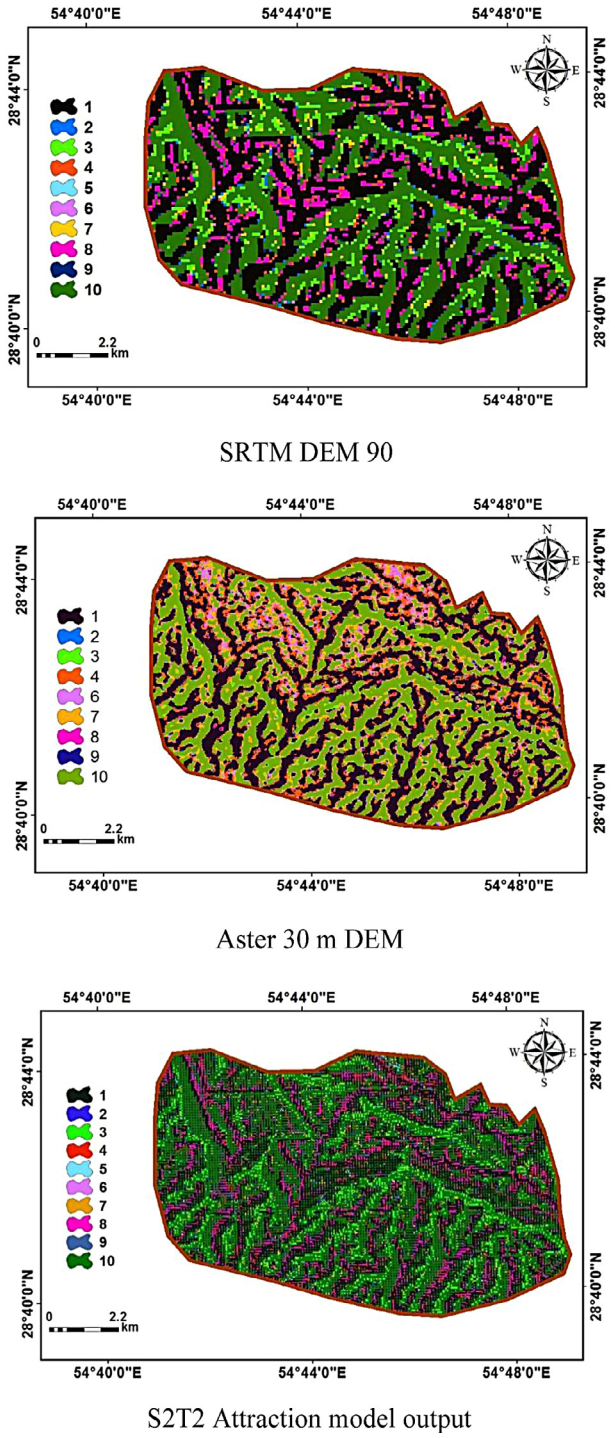

Fig. 9. Landform classification by using the attraction model, DEM 90 m of Shuttle Radar Topography Mission (SRTM) and Aster 30 m DEM (1: Canyons, deeply incised streams, 2: Mid slope drainages, shallow valleys, 3: upland drainages, headwaters, 4: U-shaped valleys, 5: Plains small, 6: Open slopes, 7: Upper slopes, mesas, 8: Local ridges/hills in valleys, 9: Midslope ridges, small hills in plains, 10: Mountain tops, high ridges).

each input is calculated and then they are compared with each other. Results showed that there are clearly differences between two DEMs. Therefore, all classes of Canyons, deeply incised streams, upland drainages, headwaters, Local ridges/hills in valleys (classes of 1, 3 and 9) in the attraction model are decreased whereas other classes are being increased in the attraction model than DEM 90 m.

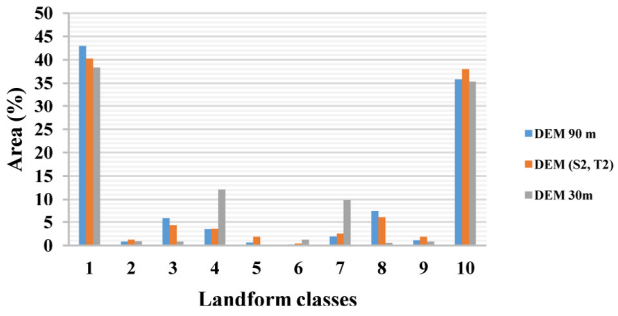

Fig. 10. The comparison of landforms extracted by three DEMs.

The values of touching method with the scale factor of 2 are the same with the quadrant method for the same scale factor due to the presence of the attraction model which caused the same neighboring pixels for scale factor of 2. With the increase in the scale factor value, the RMSE value increases as well that causes a decrease in the model accuracy. Because sub-pixel classes are estimated with higher scale factors of the attraction model, accuracy is decreased. Other scale factors cause a little raise in the RMSE values. Noticeably, since this value is not too much, it can be used due to the fine spatial resolution of the output DEMs.

In fact the lowest RMSE value belongs to S = 2, T = 1 and S = 2, T = 2 because both of these methods have the same neighborhood; therefore, their results are the same. By increasing the value of the scale factor, only one class is used in the attraction method (only elevation); therefore, at the time of setting a value to a sub-pixel in some cases (for example in sub-pixel (2, 3) in the quadrant method and scale factor of (3), more pixels are used to calculate the attraction value and accordingly the pixel with higher attraction value may be in far distance than other pixels. This results in setting a sub-pixel value to a value of pixel in far distance and decreasing the accuracy. In general, the touching neighboring method gives more accurate results because it employs fewer pixels than the quadrant method in calculating each sub-pixel.

Regarding the imperial perspective, with any increase in scale factor the accuracy of models is decreased. This fact is justified by the way by which the sub-pixel model can gather information from surrounding pixels since each sub-pixel should get a value from surrounding classes. Therefore, when the scale factor increases, the number of sub pixels in a pixel increases as well and then the way to set a value to each sub-pixel faces some inaccuracy, for example in the below image with different scale factors in the quadrant method are used and when a scale factor increases, reversely. For instance, to set the value of a sub-pixel located in (1, 1) position, three surrounding pixels are used; however, to calculate the value of a sub-pixel located in (2, 3) position in scale factor 2, all five surrounding pixels are used and since here, only one class or one elevation is used, the information in the lower scale factor is more accurate than higher ones.

In general, here with the enhancement of resolution, sub-pixel values are divided spatially and then they are recalculated. This makes them more accurate when authors use ground station points to calculate RMSE; however, when the scale factor increases more than 2, the accuracy in sub-pixels starts decreasing.

The attraction model algorithm has a few simple basic rules. The assignment of pixels is performed during a one-step process, which always yields the same output and leads to another advantage: the absence of iterations. There is no need for calibration/training as it is a case with machine learning methods, limits the computation time and results in making a relatively fast algorithm (less than 10 min with scale factor 2 for a 3601∗3601-pixel image on an Intel core i7, 1.60 GHz processor). Another advantage is its ability to deal with the soft classifications with more than two

Please cite this article in press as: Mokarrama, M., Hojati, M. Egypt. J. Remote Sensing Space Sci. (2016), http://dx.doi.org/10.1016/j.ejrs.2016.11.005

Table 3
The area of each class measured by two DEMs of the study area.

Landform class	S2, T2		DEM 90		DEM 30 m	
	Area (%)	Area (km^2)	Area (%)	Area (km^2)	Area (km^2)	Area (%)
Canyons, deeply incised streams	40.25	35.64	42.98	38.06	54.53	48.29
Mid slope drainages, shallow valleys	1.25	1.11	0.84	0.74	1.29	1.14
Upland drainages, headwaters	4.34	3.84	5.82	5.15	1.18	1.04
U-shaped valleys	3.54	3.13	3.49	3.09	17.20	15.23
Plains small	1.84	1.63	0.58	0.51	0.00	0.00
Open slopes	0.37	0.33	0.16	0.14	1.74	1.54
Upper slopes, mesas	2.54	2.25	1.90	1.68	14.03	12.42
Local ridges/hills in valleys	6.07	5.37	7.36	6.52	0.79	0.70
Midslope ridges, small hills in plains	1.85	1.64	1.09	0.97	1.18	1.04
Mountain tops, high ridges	37.97	33.62	35.77	31.67	50.25	44.50
SUM	100	88.55	100	88.55	142.19	100

classes. Besides, since there are 8 neighborhoods around each pixel, this algorithm can deal with maximum 8 different classes. The extensive comparison of different sub-pixel mapping algorithms can be the subject of another research. The sub-pixel attraction model was used by many researchers for increasing the spatial resolution of the land cover, land use and satellite image. Moreover, it is manifested that in all of them by applying the spatial resolution increasing methods, it is plausible to archive images with high spatial resolution and high information of region area (Atkinson, 2005, 1997). The algorithm was evaluated both visually and quantitatively by using the RMSE accuracy index. The resulting images showed the increased accuracy when the scale factor of 2 was used; additionally, they showed a decrease in the accuracy when higher scale factors were used. Taking the best advantages of sub-pixel methods, authors of the present paper can achieve more accuracy in some cases. It also shows that they can apply these methods on ASTER DEM and the output of 15 m DEMs could be used with an acceptable accuracy.

5. Conclusion

In this paper, the landform classification of from different spatial resolutions of DEMs was performed based on the attraction model and DEM 90 m. Concerning the obtained results, it was determined that the attraction model (S3, T2) produced higher accuracy than DEM 90 m for the landform classification. In fact, the algorithm is evaluated both visually and quantitatively using RMSE accuracy index. The basic assumption is the spatial dependence as adopted by Sulebak et al. (1997). However, the concept of the spatial dependence in this study is tested by different scale levels that results in a sub-pixel interaction. Results showed that by applying the proposed method of the spatial resolution, DEM maps can be prepared with spending lower time and cost. Indeed, high resolution DEM maps can be used to find more information from the earth surface. In the present study, a new model for increasing the spatial resolution was used. Accordingly, the present paper is considered as the first attempt to run the attraction model on DEM's. Noticeably, fine results are gained. Results show that the attraction model could be used to increase the spatial resolution and also the accuracy of the resulted DEM. The performed attraction model is modified to be able to run on DEM.

In different fields of topography study such as flooding, extraction of different indexes related to topography such as (Topographic Wetness Index) TWI, landform classification, and river extraction, and results of sub-pixel attractions on DEMs can be utilized.

Conflict of interest

There is not any direct or indirect conflict of interest in this manuscript and its data.

Acknowledgements

The authors would like to acknowledge the Organization National Cartographic Center of Iran (NCC) for their assistance during compiling the study and for providing the dataset.

References

Adediran, A.O., Parcharidis, I., Poscolieri, M., Pavlopoulos, K., 2004. Computer-assisted discrimination of morphological units on north-central Crete (Greece) by applying multivariate statistics to local relief gradients. Geomorphology 58, 357–370. http://dx.doi.org/10.1016/j.geomorph.2003.07.024.

Atkinson, P.M., 2005. Sub-pixel target mapping from soft-classified, remotely sensed imagery. Photogramm. Eng. Remote Sensing 71, 839–846.

Atkinson, P.M., 1997. Mapping sub-pixel boundaries from remotely sensed images. Innov. GIS 4, 166–180.

Burrough, P.a., van Gaans, P.F.M., MacMillan, R.a., 2000. High-resolution landform classification using fuzzy-means. Fuzzy Sets Syst. 113, 37–52. http://dx.doi.org/10.1016/S0165-0114(99)00011-1.

Dikau, R., 1989. The application of a digital relief model to landform analysis in geomorphology. In: Raper, J.F. (Ed.), Three Dimensional Applications in Geographical Information Systems. Taylor & Francis, London, pp. 51–77.

Dikau, R., Brabb, E., Mark, R., Pike, R., 1995. Morphometric landform analysis of New Mexico. Zeitschrift für Geomorphol. 101, 109–126.

Etzelmüller, B., 2000. Developments in the use of digital elevation models in periglacial geomorphology and glaciology. Phys. Geogr. 41, 35–58.

Evans, I.S., 2012. Geomorphometry and landform mapping: What is a landform? Geomorphology 137, 94–106. http://dx.doi.org/10.1016/j.geomorph.2010.09.029.

Gallant, J.C., Hutchinson, M.F., 1997. Scale dependence in terrain analysis. Math. Comput. Simul. 43, 313–321. http://dx.doi.org/10.1016/S0378-4754(97)00015-3.

Guru, D.S., Dinesh, R., 2004. Non-parametric adaptive region of support useful for corner detection: A novel approach. Pattern Recognit. 37, 165–168. http://dx.doi.org/10.1016/S0031-3203(03)00234-6.

Haile, A., Rientjes, T., 2005. Effects of LiDAR DEM resolution in flood modelling: a model sensitivity study for the city of Tegucigalpa, Honduras. Isprs Wg Iii/3, Iii/4 168–173.

Hutchinson, M.F., Dowling, T.I., 1991. A continental hydrological assessment of a new grid-based digital elevation model of Australia. Hydrol. Process. 5, 45–58. http://dx.doi.org/10.1002/hyp.3360050105.

Jenson, S.K., 1991. Applications of hydrologic information automatically extracted from digital elevation models. Hydrol. Process. 5, 31–44. http://dx.doi.org/10.1002/hyp.3360050104.

Johnston, K., Ver Hoef, J.M., Krivoruchko, K., Lucas, N., 2001. Using ArcGIS geostatistical analyst. Analysis 300, 300.

Nikolakopoulos, K.G., 2006. SRTM vs ASTER elevation products. Comparison for two regions in Crete, Greece. Int. J. Remote Sens. 27, 4819–4838. http://dx.doi.org/10.1080/01431160600835853.

Koen Mertens, L.V., 2003. Using genetic algorithms in sub-pixel mapping. Int. J. Remote Sens. 24, 4241–4247. http://dx.doi.org/10.1080/01431160310001595073.

MacMillan, R., Pettapiece, W.W., Nolan, S.C., Goddard, T.W., 2000. A generic procedure for automatically segmenting landforms into landform elements using DEMs, heuristic rules and fuzzy logic. Fuzzy Sets Syst. 113, 81–109. http://dx.doi.org/10.1016/S0165-0114(99)00014-7.

Mertens, J.C.E., Chawla, N., 2014. A custom lab-scale high resolution x-ray computed tomography system for 4D materials science. Imaging performance modeling and characterization. In: Proceedings of SPIE. The International Society for Optical Engineering. http://dx.doi.org/10.1117/12.2062638.

Mertens, K., 2008. Towards sub-pixel mapping: design and comparison of techniques.

Migoń, P., Kasprzak, M., Traczyk, A., 2013. How high-resolution DEM based on airborne LiDAR helped to reinterpret landforms: examples from the Sudetes, SW Poland. Int. Conf. Geomorphol., Int. des Géomorpholog. 22, 89–101.

Mokarram, M., Danish, S., 2015. Application of Self-Organizing Map (SOM) for Clustering of Landforms in the West of the Fars Province. Science & Technology Research Institute for Defence (STRIDE), p. 4.

Mokarram,, M., Saif, M., Danish, S., 2015. Classification of zagros mountains using multiscale analysis of digital elevation models. Malaysian J. Remote Sens. 4.

Omer, C.R., Nelson, E.J., Zundel, A.K., 2003. Impact of varied data resolution on hydraulic modeling and floodplain delineation. J. Am. Water Resour. Assoc. 39, 467–475. http://dx.doi.org/10.1111/j.1752-1688.2003.tb04399.x.

Oryan, A., Sadeghi, M.J., 1997. An epizootic of besnoitiosis in goats in Fars province of Iran. Vet. Res. Commun. 21, 559–570.

Rexer, M., Hirt, C., 2014. Comparison of free high resolution digital elevation data sets (ASTER GDEM2, SRTM v2.1/v4.1) and validation against accurate heights from the Australian National Gravity Database. Aust. J. Earth Sci. 61, 213–226. http://dx.doi.org/10.1080/08120099.2014.884983.

Rezaei, M.R., Shakoor, A., 2011. Study of some concerned factors among rural farmers of Darab City (Fars Province of Iran) based on economical geography view. Development 3, 4.

Verbeiren, Sara, Eerens, Herman, Piccard, Isabelle, Bauwens, Ides, Van Orshoven, Jos, 2008. Sub-pixel classification of SPOT-VEGETATION time series for the assessment of regional crop areas in Belgium. Int. J. Appl. Earth Obs. Geoinf. 10, 486.

Saadat, H., Bonnell, R., Sharifi, F., Mehuys, G., Namdar, M., Ale-Ebrahim, S., 2008. Landform classification from a digital elevation model and satellite imagery. Geomorphology 100, 453–464. http://dx.doi.org/10.1016/j.geomorph.2008.01.011.

Schmidt, J., Hewitt, A., 2004. Fuzzy land element classification from DTMs based on geometry and terrain position. Geoderma 121, 243–256. http://dx.doi.org/10.1016/j.geoderma.2003.10.008.

Shen, D., Wang, J., Cheng, X., Rui, Y., Ye, S., 2015. Integration of 2-D hydraulic model and high-resolution lidar-derived DEM for floodplain flow modeling. Hydrol. Earth Syst. Sci. 19, 3605–3616. http://dx.doi.org/10.5194/hess-19-3605-2015.

Sulebak, J.R., Etzelmüller, B., Sollid, J.L., 1997. Landscape regionalization by automatic classification of landform elements. Nor. Geogr. Tidsskr. 51, 35–45. http://dx.doi.org/10.1080/00291959708552362.

Takagi, M., 1998. Accuracy of digital elevation model according to spatial resolution. Int. Arch. Photogramm. Remote Sens. 32, 613–617.

Verhagen, P., Drâguţ, L., 2012. Object-based landform delineation and classification from DEMs for archaeological predictive mapping. J. Archaeol. Sci. 39, 698–703. http://dx.doi.org/10.1016/j.jas.2011.11.001.

Verhoeye, J., 2002. Land cover mapping at sub-pixel scales using linear optimization techniques. Remote Sens. Environ. 79, 96–104. http://dx.doi.org/10.1016/S0034-4257(01)00242-5.

Weiss, a, 2001. Topographic position and landforms analysis, in: Poster Presentation, ESRI User Conference, San Diego, CA. pp. 227–245. doi:http://www.jennessent.com/downloads/TPI-poster-TNC_18x22.pdf.

Wolock, D.M., McCabe, G.J., 2000. Differences in topographic characteristics computed from 100- and 1000-m resolution digital elevation model data. Hydrol. Process. 14, 987–1002. http://dx.doi.org/10.1002/(SICI)1099-1085(20000430)14:6<987::AID-HYP980>3.0.CO;2-A.

Xu, J., Hang, R., Liu, Q., 2014. Patch-based active learning (PTAL) for spectral-spatial classification on hyperspectral data. Int. J. Remote Sens. 35, 1846–1875. http://dx.doi.org/10.1080/01431161.2013.879349.

Xu, X., Zhong, Y., Zhang, L., Zhang, H., 2013. Sub-pixel mapping based on a MAP model with multiple shifted hyperspectral imagery. IEEE J. Sel. Top. Appl. Earth Obs. Remote Sens. 6, 580–593. http://dx.doi.org/10.1109/JSTARS.2012.2227246.

Please cite this article in press as: Mokarrama, M., Hojati, M. Egypt. J. Remote Sensing Space Sci. (2016), http://dx.doi.org/10.1016/j.ejrs.2016.11.005